

Uptake Is the Rate-limiting Step in the Overall Hepatic Elimination of Pravastatin at Steady-state in Rats

Masayo Yamazaki,¹ Sayoko Akiyama,¹ Ryuichiro Nishigaki,¹ and Yuichi Sugiyama^{2,3}

Received February 20, 1996; accepted July 1, 1996

Purpose. Of the HMG-CoA reductase inhibitors, the hydrophilic pravastatin has been shown to exhibit relatively specific inhibition of cholesterol synthesis in the liver. As one of the reasons for this relatively specific pharmacological activity, we demonstrated that the tissue distribution of pravastatin is limited because of its high hydrophilicity, while hepatic uptake by active transport takes place at the liver surface via a multispecific anion transporter (M. Yamazaki et al., *Am. J. Physiol.*, 264, G36-44, 1993). In this study, we examined the hepatic elimination of pravastatin at steady-state.

Methods. After i.v. infusion, the plasma concentrations of pravastatin in both arterial and hepatic venous blood were measured.

Results. The hepatic availability at steady-state exhibited a clear increase on increasing the infusion rate of pravastatin. The total hepatic elimination rate at steady-state exhibited Michaelis-Menten type saturation with the drug concentration in the capillary defined by typical mathematical models (i.e., well-stirred, parallel-tube and dispersion models), K_m and V_{max} values being comparable with those obtained from analysis of the initial uptake velocity using *in vitro* isolated hepatocytes.

Conclusions. These results indicate that overall hepatic intrinsic clearance of pravastatin at steady-state is regulated by the uptake process, followed by rapid metabolism and/or biliary excretion with minimal efflux to the circulating blood.

KEY WORDS: carrier-mediated active transport; well-stirred model; parallel-tube model; dispersion model; nonlinearity; pharmacokinetics; tissue-distribution.

¹ Department of Pharmacokinetics and Biopharmaceutics, Toho University, School of Pharmaceutical Sciences, 2-2-1, Miyama, Funabashi, Chiba 274, Japan.

² Faculty of Pharmaceutical Sciences, University of Tokyo, 7-3-1, Hongo, Bunkyo-ku, Tokyo 113, Japan.

³ To whom correspondence should be addressed.

ABBREVIATIONS: HMG-CoA; hydroxymethylglutaryl-CoA, DBSP; dibromosulphophthalein, $PS_{u,inf}$; permeability surface area product of unbound drug for the influx process, CL_{sys} ; The total systemic clearance, I; infusion rate, $C_{a,ss}$; arterial plasma concentration of drug at steady-state, $V_{h,toi}$; total hepatic elimination rate at steady-state, QB ; hepatic blood flow rate, $C_{h,v,ss}$; hepatic venous plasma concentration of drug at steady-state, CL_h ; hepatic clearance, F_h ; hepatic availability, fu ; unbound fraction in plasma, $CL_{h,int,all}$; overall hepatic intrinsic clearance, WS ; well-stirred model, PT ; parallel-tube model, \hat{C}_{ss} ; mean logarithmic concentration of drug at steady-state, DN ; dispersion number, DP ; dispersion model, K_m ; Michaelis constant, V_{max} ; maximum velocity, $C_{DP,ss}$; theoretical concentration for overall hepatic intrinsic clearance defined by the dispersion model, AIC , Akaike's information criterion, $PS_{u,eff}$; permeability surface area product of unbound drug for the efflux process, CL_{int} ; intrinsic clearance for the metabolism and/or biliary excretion of unbound drug.

INTRODUCTION

We have previously demonstrated that the initial tissue distribution of the HMG-CoA reductase inhibitor, pravastatin, is extremely restricted owing to its high hydrophilicity. However, liver, which has specific uptake mechanism(s) for organic anions, exhibited efficient uptake after i.v. administration to rats (1). In addition, our study using isolated rat hepatocytes revealed that the specific uptake of pravastatin was by active transport, a mechanism shared by other organic anions such as dibromosulphophthalein (DBSP) (this uptake system is the so-called "multispecific anion transporter; ref. 2) (3). This result is supported by Ziegler and Stunkel (4). Furthermore, the permeability surface area products for the influx of unbound pravastatin ($PS_{u,inf}$) evaluated in 4 different experimental systems (*in vivo*, *in vitro* liver perfusion, isolated cells and primary cultured cells) were in good agreement (3,5). These experimental results indicate that the active transport mechanism for pravastatin on the liver surface is responsible for its initial distribution into the liver and that the early-phase hepatic distribution is membrane-permeability limited.

As far as the therapeutic use of pravastatin is concerned, it is important to evaluate quantitatively the tissue (especially liver) distribution at steady-state. However, the hepatic availability at the steady-state has never been determined. Furthermore, no one has ever investigated whether the specific uptake mechanism described above is actually responsible for its selective distribution into liver, the target organ for this drug in terms of its pharmacological activity. Accurate evaluation of hepatic clearance is very important for predicting the pharmacological effect and/or side-effects of this drug, as well as changes in drug disposition during disease. The purpose of this study is to evaluate quantitatively the hepatic distribution of pravastatin at steady-state by measuring plasma concentrations in both arterial and the hepatic venous blood. Furthermore, the rate-limiting process involved in the hepatic elimination of pravastatin is also examined over a wide range of the plasma concentrations at steady-state by comparison of the kinetic parameters estimated according to the three typical mathematical models, i.e., well-stirred model (6), parallel-tube model (7) and dispersion model (8), with those previously obtained from analysis of the initial uptake velocity using isolated hepatocytes (3).

MATERIALS AND METHODS

Chemicals

[¹⁴C]Pravastatin (10.0 mCi/mmol) and unlabeled pravastatin were kindly donated by Sankyo Co. Ltd. All other chemicals are commercially available and of analytical grade.

Animals

Male Sprague-Dawley rats (250–300 g, Nisseizai, Tokyo) were used. All the animals were treated humanely and the animal experiments were carried out according to the guidelines provided by the Institutional Animal Care Committee (Faculty of Pharmaceutical Sciences, University of Tokyo).

In Vivo Constant-infusion Study

Rats were lightly anesthetized with ether and the left femoral artery and vein were cannulated with heparinized polyethylene tubing (PE-50); the bile duct was cannulated with polyethylene tubing (PE-10) and the hepatic vein was also cannulated using the method of Yokota et al. (9). [¹⁴C] Pravastatin dissolved in physiological saline was infused through the femoral vein cannula at a flow rate of 15 μl/min. The infusion rates were set at 0.1, 0.5, 2.5, 3.4, 4.3, 5.0, and 10.0 μmol/min/kg. After a certain interval, arterial blood and bile samples were collected in polyethylene tubes. To obtain plasma, blood was centrifuged at 10,000 g for 2 min in a table-top microcentrifuge (Microfuge E, Beckman Instruments, Inc., Fullerton, CA). The radioactivity in plasma samples was determined using a liquid scintillation spectrophotometer (LC6000SE, Beckman Instruments, Inc., Fullerton, CA).

Thin-layer Chromatographic Analysis

[¹⁴C] Pravastatin was extracted from plasma by mixing with acetonitrile (5-fold dilution (v/v)). After centrifugation (10,000 g, 5 min), an aliquot of supernatant was applied to a TLC plate (Kiesel gel 60 F254 (E. Merck, F.R.G.)) and developed with CHCl₃:MeOH:CH₃COOH = 9:1:1 (v/v) as the solvent system (10). After development, the concentrations of unchanged pravastatin (parent) and metabolites were determined using a Bio-Image Analyzer BAS-2000 (Fuji Photo Film Co. Ltd., Tokyo, Japan).

Determination of Plasma Protein Binding of Pravastatin

The unbound fraction of pravastatin in plasma (*f_u*) was determined by an ultrafiltration method using Amicon YMT membrane (Amicon MPS-3 system, Amicon Division, W. R. Grace & Co., Danvers, M.A.) (1). In brief, [¹⁴C] pravastatin and unlabeled pravastatin were added to plasma specimens to produce final concentrations of 0.5 ~ 1000 μM, which correspond to the *in vivo* plasma concentration of pravastatin at steady-state. These specimens were incubated at 37°C for 10 min and then centrifuged through the membrane to determine the *f_u*.

Calculation of Pharmacokinetic Parameters

The total systemic clearance (CL_{sys}) was calculated according to the following equation:

$$CL_{sys} = I/(RB \cdot C_{a,ss}) \quad (1)$$

where, I represents the infusion rate of pravastatin, C_{a,ss} is the arterial plasma concentration of parent drug 60 min after the beginning of the infusion and RB is the blood to plasma concentration ratio (0.59; ref. 1)

Total hepatic elimination rate at steady-state (*V_{h,tot}*) was calculated from the following equation:

$$V_{h,tot} = QB \cdot (C_{a,ss} - C_{hv,ss}) \cdot RB \quad (2)$$

where,

QB hepatic blood flow rate (60 ml/min/kg; ref. 11)
C_{hv,ss} hepatic venous plasma concentration of parent drug 60 min after the beginning of the infusion

Hepatic clearance (CL_h) and hepatic availability (F_h) were calculated from the following equations, respectively:

$$CL_h = V_{h,tot}/(RB \cdot C_{a,ss}) \quad (3)$$

$$F_h = C_{hv,ss}/C_{a,ss} \quad (4)$$

MODEL-DEPENDENT ANALYSIS

[1] Well-stirred Model and Parallel-tube Model

On the basis of two typical mathematical models, *i.e.*, well-stirred model (6) and parallel-tube model (7), hepatic availability (F_h) were described as the following equations:

$$F_h = QB/(QB + f_u \cdot CL_{h,int,all WS}/RB) \quad (5)$$

$$F_h = \exp(-f_u \cdot CL_{h,int,all PT}/QB/RB) \quad (6)$$

where *f_u* is the unbound fraction of pravastatin, CL_{h,int,all} means the overall hepatic intrinsic clearance calculated as follows:

$$CL_{h,int,all WS} = V_{h,tot}/(f_u \cdot C_{hv,ss}) \quad (7)$$

$$CL_{h,int,all PT} = V_{h,tot}/(f_u \cdot \hat{C}_{ss}) \quad (8)$$

where the subscripts CL_{h,int,all} (WS and PT) mean "well-stirred model" and "parallel-tube model", respectively, and \hat{C}_{ss} represents the mean logarithmic concentration of parent drug 60 min after the beginning of the infusion as described below (7);

$$\hat{C}_{ss} = (C_{a,ss} - C_{hv,ss})/\ln(C_{a,ss}/C_{hv,ss}) \quad (9)$$

[2] Dispersion Model

According to the dispersion model (8), hepatic availability (F_h) can be described by the following equation:

$$F_h = 4a/[(1 + a)^2 \cdot \exp\{(a - 1)/2DN\} \quad (10)$$

$$-(1 - a)^2 \cdot \exp\{-(a + 1)/2DN\}]$$

where,

$$a = (1 + 4RN \cdot DN)^{1/2} \quad (11)$$

$$RN = f_u \cdot CL_{h,int,all DP}/QB/RB \quad (12)$$

DN is the dispersion number. In the analysis employing the dispersion model, a DN of 0.17 was used (8). The subscript DP denotes the dispersion model.

To estimate the CL_{h,int,all DP}, a simulation was performed. In brief, F_h was calculated using Eq. 10 by varying the CL_{h,int,all DP} over a wide range. The values of CL_{h,int,all DP} for each infusion rate were determined to see which was closest to the experimentally obtained F_h.

[3] Determination of Kinetic Parameters for the Overall Hepatic Intrinsic Clearance Defined by the Three Different Models

The kinetic parameters of the total hepatic elimination of pravastatin at steady-state were calculated as follows:

$$\begin{aligned} V_{h,tot} &= CL_{h,int,all\ WS} \cdot f_u \cdot C_{hv,ss} \\ &= \{V_{max,WS}/(K_m,WS + f_u \cdot C_{hv,ss})\} \cdot f_u \cdot C_{hv,ss} \quad (13) \end{aligned}$$

$$\begin{aligned} V_{h,tot} &= CL_{h,int,all\ PT} \cdot f_u \cdot \hat{C}_{ss} \\ &= \{V_{max,PT}/(K_m,PT + f_u \cdot \hat{C}_{ss})\} \cdot f_u \cdot \hat{C}_{ss} \quad (14) \end{aligned}$$

$$\begin{aligned} V_{h,tot} &= CL_{h,int,all\ DP} \cdot f_u \cdot C_{DP,ss} \\ &= \{V_{max,DP}/(K_m,DP + f_u \cdot C_{DP,ss})\} \cdot f_u \cdot C_{DP,ss} \quad (15) \end{aligned}$$

where K_m (μM) and V_{max} (nmol/min/kg) represent the Michaelis constant and maximum velocity, respectively. $C_{DP,ss}$ is the theoretical concentration for overall hepatic intrinsic clearance defined by the dispersion model, calculated as $V_{h,tot}$ divided by $(f_u \cdot CL_{h,int,all\ DP})$, where $CL_{h,int,all\ DP}$ was obtained as described above.

K_m and V_{max} values for each models were obtained by fitting Eqs. 13–15 to the data using the weighted non-linear least-squares method (12). The input data were weighted as the reciprocal of the square of the observed values, and the algorithm used for the fitting was the Damping Gauss Newton Method (12). AIC and final ss values were used to judge the appropriateness of the models (13).

RESULTS

The plasma concentrations of pravastatin reached a plateau approx. 40 min after the beginning of the intravenous infusion, 0.1–10.0 $\mu\text{mol}/\text{min}/\text{kg}$, having reached steady state (data not shown). Figure 1(a) shows the total systemic clearance (CL_{sys}) defined as infusion rate divided by the arterial blood concentration of pravastatin at steady-state (60 min after the beginning of infusion) (Eq. 1). CL_{sys} remained constant (50 ~ 70 ml/min/kg) at $C_{a,ss}$ 3.5 ~ 120 μM (infusion rate: 0.1 ~ 4.3 $\mu\text{mol}/\text{min}/\text{kg}$), but fell significantly to approx. 15 ml/min/kg when $C_{a,ss}$ was >340 μM . The ratio of CL_h versus CL_{sys} is shown in Fig. 1(b). At the lowest $C_{a,ss}$, the ratio was approx. 1, and as $C_{a,ss}$ increased to 340 μM , the ratio became >0.75. At the highest $C_{a,ss}$ (670 μM), the ratio fell to about 0.5.

Plasma protein binding of pravastatin did not vary significantly over a wide range of concentration (0.5 ~ 1000 μM), and the f_u was 0.67 ± 0.01 (mean \pm S.E.). Thus, we adopted 0.67 as the f_u value for all the calculations described below.

The hepatic availability (F_h) was plotted against the four different plasma concentrations of pravastatin, i.e., $C_{a,ss}$, $C_{hv,ss}$, \hat{C}_{ss} and $C_{DP,ss}$ (Fig. 2). At the lowest $C_{a,ss}$ (3.5 μM), F_h was 0.05. The hepatic availability exhibited a marked increase at the pravastatin concentrations >120 μM for $C_{a,ss}$, > 30 μM for $C_{hv,ss}$, >60 μM for \hat{C}_{ss} , and >50 μM for $C_{DP,ss}$ reaching 0.8 at the highest $C_{a,ss}$ (670 μM).

The total hepatic elimination rate shows Michaelis-Menten type saturation with $C_{hv,ss}$, \hat{C}_{ss} and $C_{DP,ss}$ (Fig. 3) and thus we estimated the K_m and V_{max} values describing the $CL_{h,int,all}$ for each model. The results are shown in Table 1. By comparison with the kinetic parameters obtained in the initial *in vitro* uptake

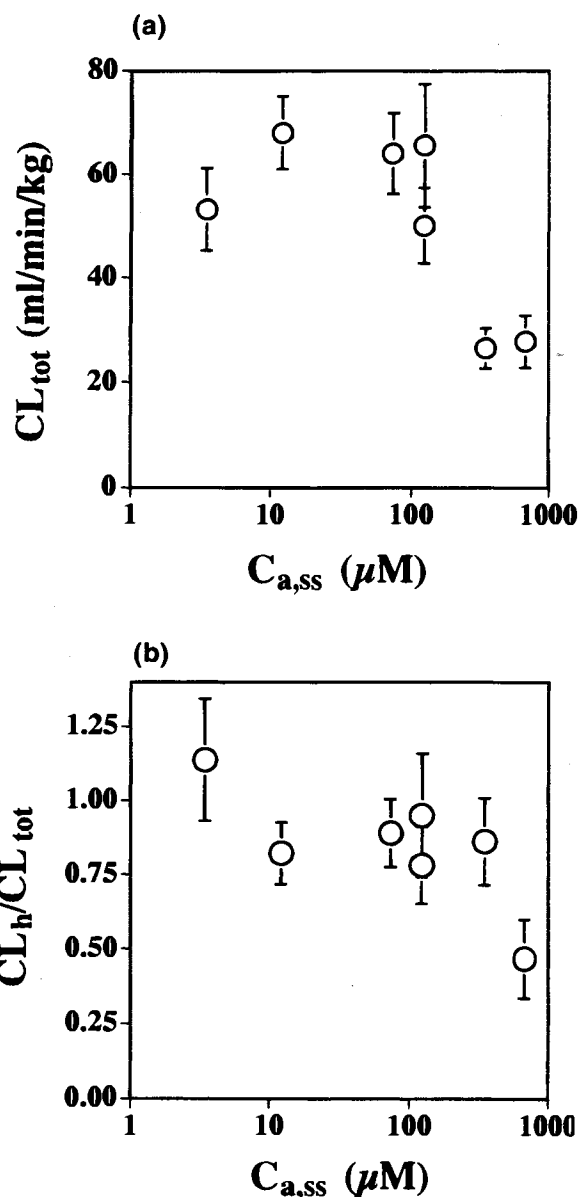


Fig. 1. (a) Dose-dependence of the total systemic clearance (CL_{sys}) of pravastatin at steady-state (60 min after the beginning of the intravenous infusion) in rats. Pravastatin was infused at 0.1, 0.5, 2.5, 3.4, 4.3, 5.0 and 10.0 $\mu\text{mol}/\text{min}/\text{kg}$. CL_{sys} was calculated from Eq. 1. Each point and vertical bar represent the mean \pm S.E. of 3 rats. (b) Dose-dependence of the hepatic clearance (CL_h) with respect to total systemic clearance (CL_{sys}) ratio of pravastatin at steady-state. CL_h was calculated from Eq. 3. Each point and vertical bar represent the mean \pm S.E. of 3 rats.

study using isolated rat hepatocytes listed in Table 1, it is obvious that there is good agreement between the kinetic parameters in the *in vitro* (initial uptake experiments) and *in vivo* (steady-state) situations. Of the models investigated, better fits were obtained from the analyses using the parallel-tube model and dispersion model compared with that of well-stirred model, as judged by the AIC and final ss values.

DISCUSSION

The total systemic clearance of pravastatin was non-linear (Fig. 1(a)). Under linear conditions ($C_{a,ss}$: 3.5 ~ 120 μM),

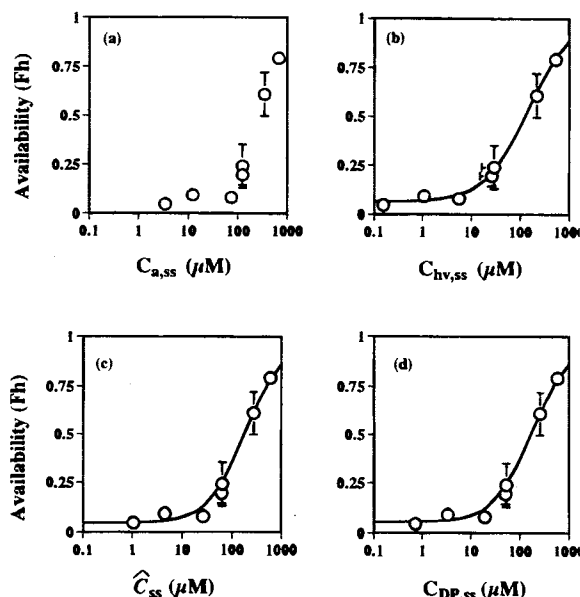


Fig. 2. Dose-dependence of the hepatic availability (F_h) of pravastatin at steady-state. F_h calculated from Eqs. 4–6 and 10 was plotted against (a) the arterial plasma concentration ($C_{a,ss}$), (b) the hepatic venous plasma concentration ($C_{hv,ss}$) (c) the mean logarithmic concentration (\hat{C}_{ss}) (Eq. 9) and (d) the theoretical concentration for overall hepatic intrinsic clearance defined by the dispersion model ($C_{DP,ss}$). Each point and vertical bar represent the mean \pm S.E. of 3 rats. The solid lines in (b), (c) and (d) were calculated from Eqs. 5, 6 and 10, using the corresponding $CL_{h,int,all}$ values obtained by fitting the data to Eqs. 13–15, using the MULTI program (12).

CL_{sys} remained constant around 50 ~ 70 ml/min/kg, which is similar to the hepatic blood flow rate (11). At the lowest $C_{a,ss}$ (3.5 μ M), the CL_h/CL_{sys} ratio was approx. 1, and as $C_{a,ss}$ increased up to 340 μ M, the ratio became >0.75 (Fig. 1(b)), indicating that hepatic elimination is the predominant route for pravastatin removal at steady-state. At the highest $C_{a,ss}$ (670 μ M), the ratio decreased to about 0.5. This phenomenon indicates that the hepatic removal was almost saturated, and, thus the contribution of non-hepatic elimination, such as urinary excretion, may increase. Or, it might be caused by saturation

of renal reabsorption. The urinary excretion of pravastatin in rats is low (~5%; 72 hr after i.v. administration of 20 mg/kg; 14), however, the initial tissue uptake clearance (in ml/min/g tissue) of kidney determined by *in vivo* integration plot analysis was approx. 60 % that of liver (1). These results suggest extensive renal reabsorption of pravastatin and saturation of reabsorption at the highest $C_{a,ss}$ in the present study. This hypothesis requires further investigation.

The hepatic availability was 0.05 at the lowest $C_{a,ss}$ (3.5 μ M) and below 0.25 at $C_{a,ss}$ values up to 120 μ M (Fig. 2). Considering the therapeutic plasma concentration of pravastatin ($>0.3 \mu$ M; 15), it is obvious that at therapeutic concentrations its hepatic extraction ratio is almost 1 and this possibly contributes to its relatively selective inhibition of hepatic cholesterol synthesis.

The hepatic elimination rate exhibited Michaelis-Menten type saturation in terms of $C_{hv,ss}$, \hat{C}_{ss} and $C_{DP,ss}$ of pravastatin (Fig. 3). The kinetic parameters obtained were comparable with those estimated from analysis of the initial rate of uptake using *in vitro* isolated hepatocytes (Table 1). These results indicate that overall hepatic intrinsic clearance ($CL_{h,int,all}$) is regulated by a saturable uptake process, which was identified *in vitro* isolated hepatocytes (3). This can be explained as follows:

Clearance concepts (16,17) are generally based on a rapid equilibrium in the distribution of drugs between blood and cells. However, this assumption does not hold for 4-methylumbelliferone (18) or even for such a lipophilic drug as *l*-propranolol (19). In these cases, the overall intrinsic clearance ($CL_{h,int,all}$) can be described by the following equation:

$$CL_{h,int,all} = PS_{u,inf} \cdot \{CL_{int}/(PS_{u,eff} + CL_{int})\} \quad (16)$$

where, $PS_{u,eff}$ represents the permeability surface area product of unbound drug for the efflux process and CL_{int} represents the "exact" intrinsic clearance for the metabolism and/or biliary excretion of unbound drug. As shown in Eq. 16, the rate-limiting step in $CL_{h,int,all}$ depends on the relative values of $PS_{u,eff}$ and CL_{int} . If $PS_{u,eff}$ is much smaller than CL_{int} ($PS_{u,eff} \ll CL_{int}$), Eq. 16 gives

$$CL_{h,int,all} = PS_{u,inf} \quad (17)$$

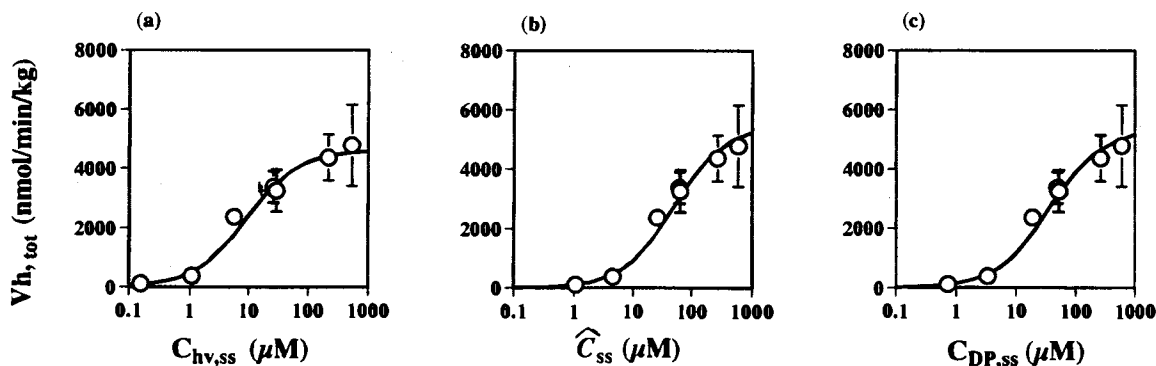


Fig. 3. Dose-dependence of the hepatic elimination rate ($V_{h,tot}$) of pravastatin at steady-state. $V_{h,tot}$ calculated from Eq. 2, was plotted against (a) hepatic venous plasma concentration ($C_{hv,ss}$), (b) mean logarithmic concentration (\hat{C}_{ss}) and (c) the theoretical concentration for overall hepatic intrinsic clearance defined by the dispersion model ($C_{DP,ss}$). The solid lines were obtained by fitting the data to (a) Eq. 13, (b) Eq. 14 and (c) Eq. 15, using the MULTI program (12). Each point and vertical bar represent the mean \pm S.E. of 3 rats.

Table 1. Comparison of the Kinetic Parameters for Pravastatin Evaluated by Means of an *In Vivo* Infusion Study (at steady-state) and *In Vitro* Isolated Cells (the initial uptake)

	K_m^a	V_{max}^b	V_{max}^c	V_{max}/K_m^d	AIC	Final SS
<i>in vivo</i> ^e						
well-stirred model (hepatic vein conc. based)	6.0 ± 1.3*	4620 ± 599*	115	19	-5.59	0.253
parallel-tube model (mean logarithmic conc. based)	33.6 ± 4.7**	5510 ± 490**	164	4.9	-12.47	0.010
dispersion model	23.3 ± 3.8***	5270 ± 499***	132	5.7	-11.97	0.102
<i>in vitro isolated cells</i> ^f	29		70	2.4		

Note: * Mean ± computer-calculated S.D. obtained by fitting the data to Eq. 13; ** Mean ± computer-calculated S.D. obtained by fitting the data to Eq. 14; *** Mean ± computer-calculated S.D. obtained by fitting the data to Eq. 15.

^a In μM . (mean ± calculated S.D.)

^b In nmol/min/kg. (mean ± calculated S.D.)

^c In nmol/min/g liver, assuming 40 g liver/kg.

^d In ml/min/g liver.

^e Present study.

^f From ref. 3.

Equation 17 indicates that only the influx process influences $CL_{h,int,all}$. The present study demonstrated practically that Eq. 17 holds for the hepatic clearance of pravastatin at steady-state, since pravastatin was efficiently taken up by an active transport mechanism followed by rapid metabolism and/or biliary excretion with minimal efflux to the circulating blood, and the $CL_{h,int,all}$ for pravastatin was regulated by the uptake process. Pravastatin is a typical drug cleared by the liver, which is the target organ for its pharmacological effect as well as the major organ regulating its pharmacokinetics in the body and this clearance is governed mainly by an uptake process which is mediated by active transport.

We have neglected the intestinal clearance of pravastatin from blood in the calculation of the hepatic elimination rate for the following reason. We previously evaluated the initial uptake clearance by integration plot analysis for several organs including liver, kidney, intestine, lung, etc. after i.v. bolus administration to rats (1). As a result, liver exhibited the greatest value (22.8 ml/min/kg), followed by kidney (2.4 ml/min/kg). As far as other organs were concerned, no significant uptake was observed (for intestine; 0.72 ml/min/kg and for lung; 0.13 ml/min/kg). Considering that the CL_{organ} at steady-state should be less than or at most equal to CL_{uptake} (20), the intestinal clearance at steady-state should be less than 0.72 ml/min/kg and intestinal clearance from blood can be neglected in the calculation of hepatic elimination rate.

We previously performed a single-pass liver perfusion study (21). In that study, the extraction ratio was 0.7 when the infusate concentration was kept at 1 μM with a flow rate of 100 ml/min/kg (no RBC condition). We can compare these values with those obtained in the present study, at least at the lowest infusion rate ($C_p = 3.5 \mu\text{M}$), taking the difference in the hepatic flow rate (100 ml/min/kg as the plasma flow in the perfusion system vs. 60 ml/min/kg as the blood flow for *in vivo* calculations) into consideration. With the extraction ratio obtained in the liver perfusion study (0.7), we can calculate the $CL_{h,int,all}$ based on the three mathematical models with the flow rate (100 ml/min/kg) and the unbound fraction in the

perfusate (0.58, ref. 21). The resultant values for $CL_{h,int,all}$ (ml/min/kg) were 402 for well-stirred model, 208 for parallel-tube model, and 243 for dispersion model. Using these values, we can recalculate *in vivo* hepatic extraction ratio using three mathematical models, assuming 60 ml/min/kg as the hepatic blood flow rate. The values obtained are 0.88 for the well-stirred model, 0.98 for the parallel-tube model and 0.96 for the dispersion model. These values are comparable with that in the present study (0.95), indicating that the ability of the liver to remove pravastatin is comparable between the *in vivo* and in the liver perfusion system.

Strictly speaking, we cannot deny the claim that the K_m and V_{max} for uptake by hepatocytes are coincidentally similar to those obtained and that there is no evidence that uptake is rate-limiting. It is very difficult to fully demonstrate experimentally that the uptake process is the rate-limiting process. The uptake can be rate-limiting when the intracellular sequestration rate (metabolism + biliary excretion) is much larger than the efflux rate (19,20). Our previous MID experiment indicates the concentrated vector uptake of pravastatin ($PSu_{inf} \gg PSu_{eff}$), suggesting the minimal efflux. This was reflected by the steady increase in the "ratio plot" with time (5). In addition, our recent biochemical and kinetic studies clarified the presence of very efficient biliary excretion system for pravastatin, which is mediated by a primary active transporter, termed canalicular multi-specific organic anion transporter (cMOAT) (M. Yamazaki et al., submitted to J. Pharmacol. Exp. Ther.). These findings may suggest once the pravastatin molecules are taken up by the hepatocytes, most of them may be excreted into the bile rather than being effluxed. In addition, our present analysis indicates that the K_m , V_{max} values for uptake by hepatocytes are similar to those obtained by the steady-state elimination *in vivo*. Taken together, we suggest that the hepatic uptake process may be a rate-limiting process of the overall hepatic elimination of pravastatin, though this may not be a definite demonstration.

In conclusion, overall hepatic intrinsic clearance of pravastatin at steady-state is regulated by the uptake process, since pravastatin was efficiently taken up by an active transport mech-

anism, which was identified using *in vitro* isolated hepatocytes, followed by rapid metabolism and/or biliary excretion with minimal efflux to the circulating blood.

ACKNOWLEDGMENTS

We would like to appreciate Sankyo Co., Ltd., for providing labeled and unlabeled pravastatin. This study was supported in part by a Grant-in-Aid for Scientific Research provided by the Ministry of Education, Science and Culture of Japan.

REFERENCES

1. M. Yamazaki, T. Tokui, M. Ishigami, and Y. Sugiyama, *Biopharm. Drug Disposit.*, in press
2. P. J. Meier, *Seminars in Liver Disease*, **8**:293-307, (1988).
3. M. Yamazaki, H. Suzuki, M. Hanano, T. Tokui, T. Komai, and Y. Sugiyama, *Am. J. Physiol.*, **264**:G36-G44, (1993).
4. K. Ziegler, and W. Stunkel, *Biochim. Biophys. Acta.* **1139**:203-209, (1992).
5. M. Ishigami, T. Tokui, T. Komai, K. Tsukahara, M. Yamazaki, and Y. Sugiyama; *Pharm. Res.*, **12**:1741-1745, (1995).
6. K. S. Pang, and M. Rowland, I: *J. Pharmacokin. Biopharm.*, **5**:625-653, (1977).
7. K. Winkler, S. Keiding, and N. Trgstrup, ed. by G. Paumgartner and R. Preisig. Basel, Karger, 1973, 144-155.
8. M. S. Roberts, and M. Rowland, *J. Pharmacokin. Biopharm.*, **14**:261-288 (1986).
9. M. Yokota, T. Iga, S. Awazu, and M. Hanano. *J. Appl. Physiol.* **4**:349-441, (1976).
10. S. Muramatsu, K. Miyaguchi, H. Iwabuchi, Y. Matsushita, T. Nakamura, T. Kinoshita, M. Tanaka, and H. Takahagi, *XENOBIOTICA*, **22**:487-498 (1992).
11. R. J. Dedrick, D. S. Zaharko, and R. Lutz, *J. Pharm. Sci.*, **62**:662-690, (1973).
12. K. Yamaoka, Y. Tanigawara, Y. Nakagawa and T. Uno. *J. Pharmacobio-Dyn.*, **4**:879-885, (1981).
13. K. Yamaoka, T. Nakazawa, and T. Uno, *J. Pharmacokin. Biopharm.*, **6**:165-175, (1978).
14. T. Komai, K. Kawai, T. Tokui, Y. Tokui, C. Kuroiwa, E. Shigehara and M. Tanaka, *Eur. J. Drug Met. Pharmacokin.* **17**:103-113, (1992).
15. Y. Tsujita, and Y. Watanabe, *Cardiovasc. Drug Rev.*, **7**:110-126, (1989).
16. M. Rowland, L. Z. Benet, and G. G. Graham, *J. Pharmacokin. Biopharm.*, **1**:123-136, (1973).
17. G. R. Wilkinson, and D. G. Shand, *Clin. Pharmacol. Ther.*, **18**:377-390, (1975).
18. S. Miyauchi, Y. Sugiyama, Y. Sawada, K. Morita, T. Iga, and M. Hanano, *J. Pharmacokin. Biopharm.*, **15**:25-38, (1987).
19. S. Miyauchi, Y. Sawada, T. Iga, M. Hanano, and Y. Sugiyama, *Biol. Pharm. Bull.*, **16**:1019-1024 (1993).
20. M. Yamazaki, H. Suzuki and Y. Sugiyama, *Pharm. Res.*, **13**:497-513, (1996).
21. M. Yamazaki, K. Kobayashi and Y. Sugiyama, in *Biopharm. Drug Disposit.*, in press.